

Concentration Dependent Structural, Optical and Electrochromic Properties of MoO₃ Thin Films

S.S. Mahajan¹, S.H. Mujawar², P.S. Shinde², A.I. Inamdar², P.S. Patil^{2,*}

¹ Jaysingpur college Jaysingpur, India

² Thin Films Materials Laboratory, Department of Physics, Shivaji University, Kolhapur- 416 004, Maharashtra, India

*E-mail: psp_phy@unishivaji.ac.in

Received: 12 April 2008 / Accepted: 7 May 2008 / Online Published: 30 June 2008

Thin films of molybdenum trioxide were deposited onto glass and electrically conducting substrates fluorine doped tin oxide coated glass (FTO) by spray pyrolysis technique. The effect of concentration (5mM, 10mM, 15 mM) on the structural, morphological, optical and electrochromic properties of MoO₃ thin films were studied. The structural studies reveal MoO₃ orthorhombic structure of the thin films. With increase in concentration band gap energy varies from 3.11 to 3.04eV. The self-assembled thread like morphology of thin film was confirmed by AFM analysis. Diffusion constant increases with increase in solution concentration from 1.38×10^{-10} to 1.66×10^{-10} cm²/s. With increase in concentration of MoO₃ coloration efficiency increases from 10 to 19 cm²/C, whereas reversibility decreases from 71 to 63%.

Keywords: Spray pyrolysis technique. Molybdenum trioxide, thin films; Electrochromism

1. INTRODUCTION

Transition metal oxides with diverse structures, properties, and phenomena have been the focus of much attention in recent years in view of their scientific and technological applications. Molybdenum oxide (MoO₃), among the other transition metal oxides, exhibits interesting structural, chemical, electrical, and optical properties [1–12]. MoO₃ finds application as a cathode material in the development of high-energy density solid-state microbatteries [4, 5]. It is considered as a promising chromogenic/electrochromic material, as it exhibits electro-, photo-, and gaso-chromic effects by virtue of which the material is of much interest for the development of electrochromic display devices, optical switching coatings, display devices, and smart window technology [1–3,6–10]. Molybdenum oxide films and nano-crystals also find application in sensors and lubricants [11–13]. In all these

technological applications, optimization of the growth conditions to produce phase pure MoO₃ thin films with controlled structure, morphology, optical and electronic properties is important. Therefore, an understanding of the growth mechanism, microstructure formation and surface modification as a function of growth conditions is prime requisite. Understanding of the composition, structure, and phase of the grown MoO₃ films since the properties and performance of the resulting films are mainly governed by their microstructure. MoO₃ exists in polycrystalline, the thermo-dynamically stable orthorhombic α -MoO₃ phase. Synthesis of crystalline MoO₃ films requires higher temperatures, where the compositional deviation is very common resulting in the formation of layers with Mo in the reduced state [4–14]. In the present work, an attempt has been made to grow thin layers of Mo oxides using a cost effective spray pyrolysis technique. The purpose of this work is to establish and optimize the growth conditions to produce MoO₃ films for optical and electrochemical applications. The grown films were characterized by a wide variety of surface/interface analytical techniques in order to obtain the complete information on the crystal structure of film, composition, phase, and morphology. Using the results obtained and presented in this paper, we show that the stable and single-phase α -MoO₃ films, without any compositional deviation, can be grown using spray pyrolysis technique

2. EXPERIMENTAL PART

Molybdenum oxide thin films are deposited onto the glass and fluorine doped tin oxide (FTO) coated (15-20 Ω/\square) glass substrates by spray pyrolysis technique. MoO₃ powder (GR grade, Loba Chemie) was dissolved in ammonia solution at room temperature to form ammonium molybdate and doubly distilled water was added to obtain an appropriate concentration of spraying solution [15]. The precursor concentration was varied from 5-15 mM. Films deposited on glass substrates were used for structural and optical properties whereas those deposited on FTO-coated glass substrates were used for electrochromic properties. The samples deposited at various concentrations 5, 10, and 15 mM are denoted by Mo₁, Mo₂, and Mo₃ respectively.

Electrochemical measurements were performed by using potentiostat EG & G make Versastat-II (PAR 362) model controlled by personal computer (PC) in three electrode cell configuration with electrochemistry software M270. MoO₃ thin films onto FTO coated conducting glass substrate of 2 cm² area is used as a working electrode, a platinum wire as a counter electrode and saturated calomel electrode (SCE) as a reference electrode (SCE, E₀= 244 mV Vs SHE, the standard hydrogen electrode). X-ray diffraction (XRD) spectra of the films were recorded on a X-ray diffractometer (Philips PW-1710) with Cu-K α radiation of 1.5418 Å wavelength. Various thicknesses were measured by using AMBIOS make XP-1 surface profiler and are found to be 320,460, 540nm. The three dimensional morphology of the growth was examined by using atomic force microscopy (AFM), Nanoscope instruments, USA in contact mode, with V shape silicon nitride cantilever of length 100 μ m and spring constant 0.58 N/m.

3. RESULTS AND DISCUSSION

3.1. X- ray diffraction studies

The structural changes & identification of phases were studied with the help of XRD technique. The diffracting angle θ - 2θ was varied between 10 & 50°. Figure 1 show XRD patterns for Mo₁, Mo₂, and Mo₃ samples. The observed XRD patterns were compared with standard JCPDS card (file numbers: 35 – 508). Films are polycrystalline with well-defined diffraction peaks along (0 2k 0) reflections with k= 1, 2 and 3. The good agreement of 'd' values with standard data indicates that the films consist of MoO₃ with α -orthorhombic structure. The XRD patterns of the samples manifest that (040) plane appears with relatively higher intensity. Besides this minor peak along (021) plane is also observed. The grain size were calculated to be 45, 47, 45nm for sample Mo₁, Mo₂, and Mo₃ respectively. It is seen from the figure that the film crystallinity ameliorates with increase in solution concentration owing to increment in crystal size.

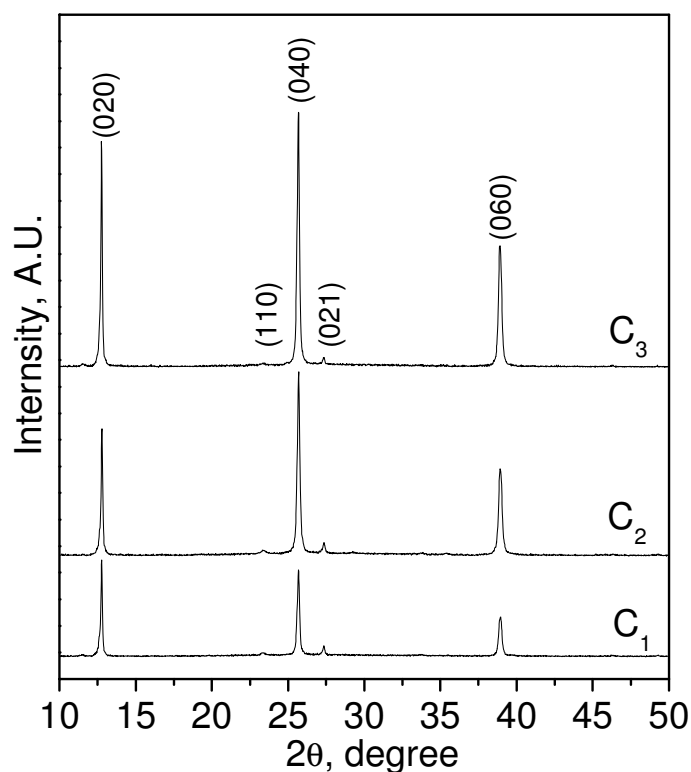


Figure 1. X-ray diffraction patterns of MoO₃ thin films deposited at different solution concentrations: 5 mM (Mo₁), 10 mM (Mo₂) and 15 mM (Mo₃); the substrates temperature was 350°C.

3.2. Atomic force microscopy (AFM)

Fig. 2 shows the 3D atomic force microscope images recorded for the samples Mo₁, Mo₂, and. It is obvious from these images that with increase in solution concentration, the grain size increases.

The average grain sizes for the samples Mo₁, Mo₂, and Mo₃ are respectively in the range 300-450 nm, 500-650 nm and 600-750 nm. Agglomeration of grains to form relatively flat uniform surface was observed for Mo₃ sample. Such flat rectangular grains render well aligned crystalline (0 2k l) oriented MoO₃ films.

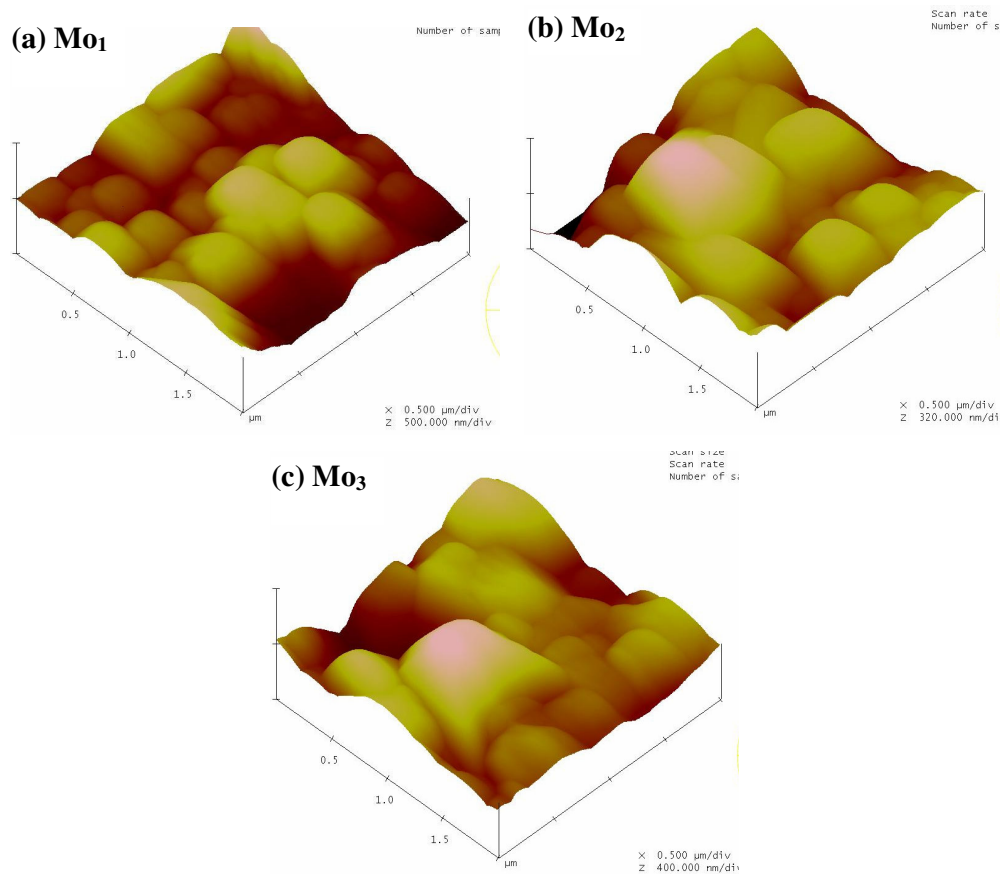


Figure 2. Atomic force microscope images for samples Mo₁, Mo₂, and Mo₃.

3.3. Electrochemical Measurement

The simultaneous electrochemical intercalation and deintercalation of electrons and H⁺ ions were carried out using a solution of 0.5M of H₂SO₄ electrolyte solution with graphite as counter electrode and saturated calomel as a reference electrode.

3.4. Cyclic Voltammograms (CV)

Figure 3. shows cyclic voltammograms recorded for all the samples Mo₁, Mo₂, and Mo₃ after first cycle with linear potential sweep between -400 to +400 mV (versus SCE) at fixed scan rate 50 mV/s. Upon reversal of the potential scan, anodic current wave with broad peak centered at -200 mV

(versus SCE) was observed for sample Mo₃. The CV spectra for all the samples display different area under the curves. Thus it is inferred that all the samples undergo reduction-oxidation processes. However, MoO₃ sample has suitable host matrix with adequate mixed ionic conductivity for easy intercalation and de-intercalation of the ions. Dependence of peak current densities with scan rate can well be understood from figure 3 wherein peak current densities (both anodic and cathodic) are plotted as a function of square root of scan rate for all three samples Mo₁, Mo₂, and Mo₃. This plot reflects the nature of reaction kinetics. A linear relationship implies that the reaction is diffusion controlled. Magnitude of diffusion depends critically on nature of diffusing ionic species, crystallinity, porosity, hydration of the host lattice and type of electrolyte. The diffusion coefficient of H⁺ ions during intercalation and deintercalation is calculated by using Randles -Servcik equation (1).

$$D^{1/2} = \frac{i_p}{2.72 \times 10^5 \times n^{3/2} \times A \times C_0 \times \nu^{1/2}} \text{----- (1)}$$

From the slope of the curve of the cathodic/ anodic peak current verse square root of scan rates in the linear part, the diffusion coefficient calculated and found to be 1.38×10^{-10} and 1.66×10^{-10} cm²/s for intercalation and de- intercalation process, respectively. The cycle life is a measure of the number of repetitive color-bleach cycles, which the film can sustain without degradation. The stability of the samples in 0.5M H₂SO₄ electrolyte is tested by repeating color-bleach cycles between -400 to +400 mV several times. The stability of the samples in 0.5M H₂SO₄ electrolyte is tested by repeating color-bleach cycles between -500 to +500 mV several times.

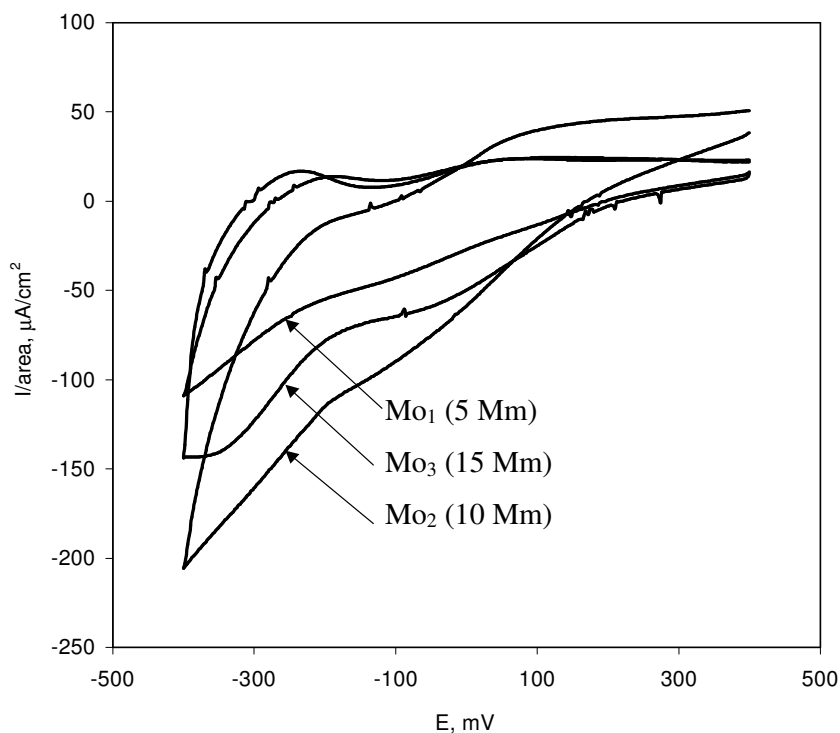


Figure 3. Overlays of cyclic voltammograms (CV) recorded (vs. SCE) at the scan rate of 50 mV/sec all the samples Mo₁, Mo₂, and Mo₃.

The response time for coloration (t_c) and bleaching (t_b) was calculated from current time transient data and shows very fast color-bleach kinetics which is shown in the table 1. The bleaching kinetics is always faster than the coloring rate for MoO₃ films owing to the well-defined different mechanisms controlling the two processes. The bleaching speed is governed by the space charge limited current flow of cations through the bulk of the film whereas in the coloring mode the potential barrier at the MoO₃ – electrolyte interface and the number of H⁺ intercalation play a critical role. The amount of H⁺ ions intercalation and deintercalation with respect to time was carried by using chronocoulometry (CC) studies, (table 1) which can further be used to estimate reversibility, and coloration efficiency.

Table 1.

Sample Code	Response time		Q _i (□C/cm ²)	Q _{di} (□C/cm ²)	Reversibility %
	(t _c) sec	(t _b) sec			
C ₁	7.2	5.2	944	682	71%
C ₂	6.4	4.4	1192	812	68%
C ₃	5.2	3.9	1886	1595	63%

Table 2.

Sample Code	T _b %	T _c %	(ΔOD) _{630nm}	Coloration efficiency cm ² /C
C ₁	81	73	1.04	10
C ₂	82	71	1.44	12
C ₃	58	39	3.64	19

3.5. Optical Transmission

The dependence of optical transmittance in the wavelength of 350 to 850nm for the bleached and the colored MoO₃ thin films shown in Figure 4. The maximum transmittance observed for bleached film is ~80% at peak position wavelength 630 nm. The transmittance observed for the colored film was 73% for the sample C₁. The coloration efficiency (η) at a particular wavelength correlates with the optical contrast, i.e. the change in optical density with charges intercalated per unit electrode area (q/A) and can be expressed by equation (2).

$$\eta = \frac{\Delta OD_{\lambda}}{Q_i} = \frac{\log(T_b / T_c)}{q / A} \text{ ----- (2)}$$

where T_b and T_c are the transmittances of the film in the bleached and colored states, respectively. But the maximum colouration efficiency (η) was observed for C₃ sample 19%. The transmittance observed for the colored film is 58%. The transmittance observed for the bleached film 39%. The coloration

efficiency was determined for sample by injecting 6.88 mC/cm^2 charges in the film and have been plotted as a function of the wavelength in the 350 - 850 nm range shown in Figure 4. The coloration efficiency at 630nm is 19%.

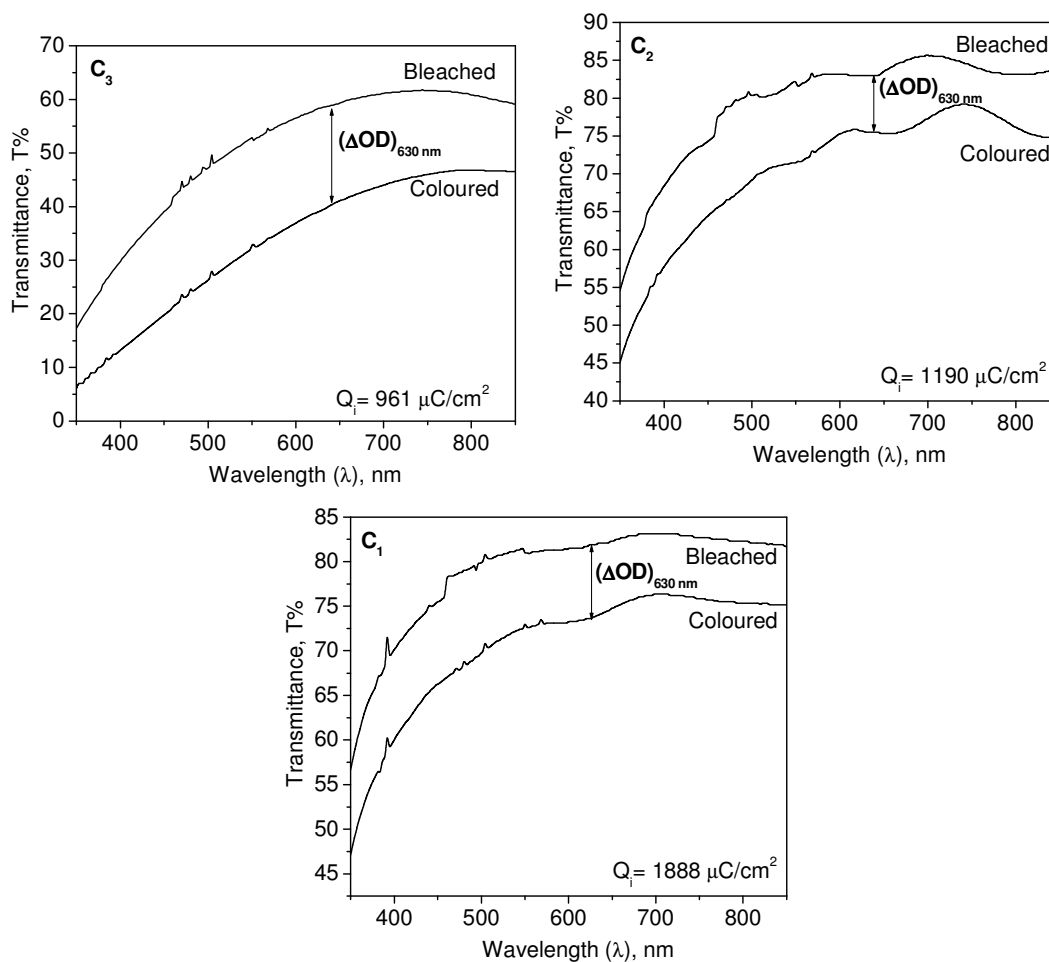


Figure 4. The plots of Transmittance (%T) versus wavelength for as-deposited samples Mo₁, Mo₂, and Mo₃ in colored and bleached states. The coloration and bleaching voltages were -0.4V (SCE) and +0.4V(SCE) respectively for 10 sec.

4. CONCLUSIONS

Molybdenum trioxide thin films were successfully deposited at various solution concentrations. The crystallite size is varied 45, 47, 45 nm for concentration 5mM, 10 mM, 15 mM respectively. The self-assembled thread like morphology of thin film confirm by AFM analysis. Diffusion constant increases with increases solution concentration. Diffusion constant varies from 1.38×10^{-10} to $1.66 \times 10^{-10} \text{ cm}^2/\text{s}$. The coloration was found to be associated with H⁺ ion intercalation. Coloration efficiency was varied from 10% to 19% observed at 630nm due to porous nature of the films. The electrochromic

properties (CV, CA, and CC) confirm the very fast color-bleach kinetics, stability and good reversibility.

ACKNOWLEDGEMENTS

The authors wish to acknowledge the U.G.C., New Delhi for the financial support through the DST, through FIST (2002-2007) program and UGC-ASIST (2005-2010) program.

References

1. C.G.Granqvist, Handbook of Inorganic Electrochromic Materials, Elsevier, 115.
2. T.S.Sian, G.B.Reddy, *Appl.Surf.Sci.*236 (2004) 1.
3. S.H.Lee, M.J.Seong, C.E.Tracy, A.Mascarenhas, J.R.Pitts, S.K.Deb, *Solid State* 147 (2002) 129.
4. C.Julien in: G.Pistoria (Ed.), Lithium Batteries: New Materials, Developments and Perspectives, Amsterdam, North-Holland, 1994.
5. W.Li, F.Cheng, Z.Tao, J.Chen, *J.Phys.Chem.B* 110 (2006) 119.
6. T.S. Sian, D.B.Reddy, *J.Appl.Phys.* 98 (2005) 026104.
7. V.Bhosale, A.Tiwari, J.Narayan, *J.Appl.Phys.*97 (2005) 083539.
8. K.Gesheva, M.Surtchev, T.Ivanova, *Solar Energy Mater. Solar Cell* 76 (2003) 563.
9. J.N.Yao.Y.A.Yang, B.H.Loo, *J.Phys.Chem. B* 102 (1998) 59.
10. J.Okumu, F.Koerfer, C.Salinga, M.Wuttig, *J.Appl.Phys.* 95 (2004) 7632.
11. A.K.Prasad, D.J.Kubinski, P.I.Gouma, *Sents.Actuators B* 93 (2003) 25.
12. K.Hosomo, I.Matsubara, N.Murayama, S.Woosuck, N.Izu, *Chem.Mater.*17 (2005) 349.
13. J.Wang, K.C.Rose, C.M.Lieber, *J.Phys.Chem.B* 103 (1999) 8405.
14. C.Julien,A.Kheifa,O.M.Hussain,G.A.Nazari,*J.Cryst.Growth* 156 (1995) 235.
15. P. S. Patil and R. S. Patil *Bull. Mater. Sci.* 18 (1995) 911